J Digit Imaging (2013) 26:1001–1007
DOI 10.1007/s10278-013-9595-6

Optimization of Computed Tomography Protocols: Limitations of a Methodology Employing a Phantom with Location-Known Opacities

Karen L. Dobeli · Sarah J. Lewis · Steven R. Meikle · David L. Thiele · Patrick C. Brennan

Published online: 14 May 2013

Abstract This study aimed to determine if phantom-based methodologies for optimization of hepatic lesion detection with computed tomography (CT) require randomization of lesion placement and inclusion of normal images. A phantom containing fixed opacities of varying size (diameters, 2.4, 4.8, and 9.5 mm) was scanned at various exposure and slice thickness settings. Two image sets were compared: All images in the first image set contained opacities with known location; the second image set contained images with opacities in random locations. Following Institutional Review Board approval, nine experienced observers scored opacity visualization using a 4-point confidence scale. Comparisons between image sets were performed using Spearman, Kappa, and Wilcoxon techniques. Observer scores demonstrated strong correlation between both approaches when all opacity sizes were combined (r=0.92, p<0.0001), for the 9.5 mm opacity (r=0.96, p<0.0001) and for the 2.4 mm opacity (r=0.64, p<0.05). There was no significant correlation for the 4.8 mm opacity. A significantly higher sensitivity score for the known compared with the unknown location was found for the 9.5 mm opacity and 4.8 mm opacity for a single slice thickness and exposure condition (p<0.05). Phantom-based optimization of CT hepatic examinations requires randomized lesion location when investigating challenging conditions; however, a standard phantom with fixed lesion location is suitable for the optimization of routine liver protocols. The development of more sophisticated phantoms or methods than those currently available is indicated for the optimization of CT protocols for diagnostic tasks involving the detection of subtle change.

Keywords Dose optimization · Radiation · Phantom · Computed tomography

K. L. Dobeli · S. J. Lewis · S. R. Meikle · P. C. Brennan
Medical Image Optimisation and Perception Group (MIOPeG), Medical Imaging & Radiation Sciences Faculty Research Group, Faculty of Health Sciences, The University of Sydney, Cumberland Campus, Lidcombe, NSW 2141, Australia

K. L. Dobeli (✉)
Department of Medical Imaging, Royal Brisbane and Women's Hospital, Level 3 Ned Hanlon Building, Butterfield St, Herston, QLD 4029, Australia
e-mail: karendobeli@bigpond.com.au

K. L. Dobeli · S. J. Lewis · S. R. Meikle · P. C. Brennan
Brain and Mind Research Institute, The University of Sydney, 100 Mallett St, Camperdown, NSW 2050, Australia

D. L. Thiele
Biomedical Technology Services, Queensland Health, 450 Gregory Terrace, Fortitude Valley, QLD 4006, Australia

Introduction

Substantial increases in computed tomography (CT) usage and population dose have been reported in the USA, UK, Europe, and Australia over the past two decades [1–5] resulting in governments, radiation regulatory bodies, and radiology associations and professionals highlighting the need for optimized CT protocols [6–8]. Establishing such protocols often involves the use of phantoms due to the difficulty of employing patients when comparing different technical or procedural factors involving ionizing radiation [9–11].

Phantoms generally consist of a cylinder of homogeneous material within which spheres or rods of different sizes and CT densities, aimed at simulating lesions, are positioned. The simulated lesions usually have fixed location and are "framed" by surrounding structures, which are

often more conspicuous than the lesion/s of interest. This is a potential limitation of a dose optimization process performed using a phantom because a priori knowledge of the presence or location of a lesion improves observer performance [12]. The optimized dose for a particular diagnostic task determined using a phantom with framed lesions might therefore be lower than the dose required for clinical examinations. Phantom methods, however, have the advantages of widespread availability and simplicity of use, but to the authors' knowledge, the effect of the use of a phantom with framed lesions on dose optimization has not been established. The purpose of this phantom-based study is to determine if phantom-based methodologies for optimization of hepatic lesion detection with CT require randomization of lesion placement.

Materials and Methods

Approval to conduct the study was granted from the study center's institutional review board for low and negligible risk research (protocol LR 09/93). Informed consent of the clinical personnel who participated as observers was obtained.

Two image sets were required for the purposes of this study: one set containing images with framed lesions typical of image sets produced with commercially available CT phantoms and a second set including images with lesions in random locations to represent the clinical situation.

A CT liver lesion phantom (Model 061, CIRS, Norfolk) was scanned at various combinations of exposure level and slice thickness using a 64-slice CT unit (Brilliance 64, Philips Medical Systems, Cleveland) (Table 1). The phantom consisted of a soft-tissue-equivalent disk containing spherical opacities of different sizes and densities, the focus here being the opacities of 9.5, 4.8, and 2.4 mm each with a density of 10 HU lower than the background. A diameter of 10 mm has been used as a size threshold for the investigation of liver lesions in a number of studies [13, 14], and the 9.5 mm sphere was close to this size. The routine use of thinner collimation with multidetector CT has resulted in more frequent detection of very small lesions [15], and the detection and characterization of small lesions can be important for patients with history of malignancy [14], hence the inclusion of the two smaller opacity sizes in this study.

Image Set One

The first image set randomly combined images that passed through the center of the opacities (Fig. 1a), thus representing the framed lesion condition. Five images for each of the 12 combinations listed in Table 1 (60 images in total) were presented.

Image Set Two

A second set of images representing random lesion location was created by loading the central images (containing opacities) and distal images (no opacities) for each of the original scan series into an image-editing program (Adobe Photoshop CS4 Extended, Adobe Systems Incorporated, USA). Regions of interest (ROIs) were placed in the central image around the opacities under investigation and copied. The copied regions of interest were randomly pasted onto the distal image (originally without opacities) from the same image set, the diameter of the cut area being approximately twice that of the extracted opacity and the outer three pixels of the extracted region were blended into the background image (Fig. 1). The ROIs were positioned such that the center of a pasted opacity was located at a distance from the center of the phantom equal to that of its position in the image from which it was removed.

Comparison of the minimum, maximum, average, and standard deviation of the pixel values in identical regions of interest positioned over the opacities in the edited image and in the original central image were performed, demonstrating that the editing process had not altered the appearance of the opacities or surrounding background.

The number of copied opacities embedded within a single image (minimum of one and maximum of five) was also generated via a ballot system. In total, each of the three opacity sizes (9.5, 4.8, and 2.4 mm) was presented five times for each exposure/slice thickness combination (Table 1). Sixty images (five images for each of the 12 combinations listed in Table 1) containing randomly located opacities were created and randomly combined.

Analysis

Nine observers (three consultant radiologists and six specialist CT radiographers) having between 7.5 and 20 years experience in viewing abdominal CT images reviewed both image sets in a single session after participating in a short training session. For each image in the framed opacity image set, the observers scored the visualization of the three opacity sizes under investigation using a 4-point scale, where 1=opacity not visible, 2=opacity possibly visible, 3=opacity probably visible, and 4=opacity definitely visible. For the second image set, the observers circumscribed any perceived opacities and rated their level of confidence in marking each identified opacity using the 4-point scale, described above. Images were viewed on a dedicated image review station (DS3000, Agfa), which was calibrated for each reading session to DICOM Part 4 Curve standard. Ambient lighting conditions in the viewing room were maintained throughout the study at 25–40 lx [16].

Analysis of the two image sets was performed for all opacities combined and for each opacity size individually using three methods. Firstly, differences in observer scores

Table 1 Median and mean observer scores for the three opacity sizes at each exposure/slice thickness setting: *p* value is presented when a significant difference between the two methods exists

Lesion size (mm)	Slice thickness (mm)	Exposure (mAs)	Median (mean) observer scores		*p* value
			Framed lesion location	Random lesion location	
9.5	5	125	4.00 (3.73)	4.00 (3.93)	
		100	3.80 (3.67)	3.60 (3.69)	
		75	3.60 (3.60)	3.80 (3.71)	
		50	3.60 (3.47)	3.40 (3.52)	
	3	125	3.80 (3.73)	4.00 (3.82)	
		100	3.75 (3.71)	3.80 (3.78)	
		75	3.60 (3.53)	3.40 (3.18)	
		50	3.60 (3.49)	4.00 (3.58)	
	1	125	3.60 (3.40)	3.40 (3.40)	
		100	3.00 (3.09)	3.20 (3.11)	
		75	3.00 (3.00)	1.80 (1.38)	<0.05
		50	2.80 (2.77)	2.60 (2.58)	
4.8	5	125	1.40 (1.38)	1.60 (1.53)	
		100	1.20 (1.27)	1.00 (1.00)	
		75	1.20 (1.29)	1.00 (1.09)	
		50	1.10 (1.13)	1.00 (1.11)	
	3	125	1.40 (1.38)	1.40 (1.40)	
		100	1.40 (1.29)	1.00 (1.02)	
		75	1.40 (1.31)	1.00 (1.07)	
		50	1.20 (1.36)	1.00 (1.44)	
	1	125	1.20 (1.22)	1.20 (1.16)	
		100	1.00 (1.13)	1.00 (1.02)	
		75	1.00 (1.18)	1.00 (1.09)	
		50	1.00 (1.18)	1.00 (1.04)	
2.4	5	125	1.00 (1.04)	1.00 (1.02)	
		100	1.00 (1.07)	1.00 (1.04)	
		75	1.00 (1.04)	1.00 (1.00)	
		50	1.00 (1.02)	1.00 (1.00)	
	3	125	1.00 (1.00)	1.00 (1.00)	
		100	1.00 (1.00)	1.00 (1.00)	
		75	1.00 (1.00)	1.00 (1.02)	
		50	1.00 (1.00)	1.00 (1.00)	
	1	125	1.00 (1.00)	1.00 (1.00)	
		100	1.00 (1.00)	1.00 (1.00)	
		75	1.00 (1.04)	1.00 (1.04)	
		50	1.00 (1.00)	1.00 (1.00)	

between the framed and randomly located opacities were established using the Wilcoxon matched-pairs signed rank test. Secondly, correlation of observer scores between the two image sets was performed using Spearman's rank correlation coefficient (r). Thirdly, interobserver agreements for each image set were calculated using Randolph's free-marginal kappa (K). Finally, differences in sensitivity between the framed and randomly located opacities were determined using the Wilcoxon matched-pairs signed rank test. A true positive was declared if the distance from the center of an ROI to the center of a nearby true lesion was <10 mm for the 9.5 mm opacity, or <5 mm for the two smaller opacities. These values represent the maximum distances at which overlap of a marked ROI, and the true lesion would be likely to occur considering the average diameter of the marked ROIs for the true positive findings for each lesion size, which indicated that the observers were able to accurately circumscribe the 9.5 and 4.8 mm opacities but

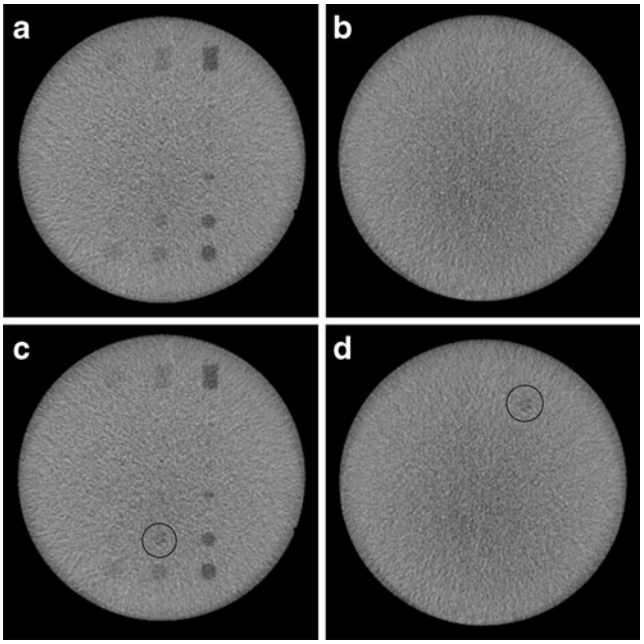

Fig. 1 Central (**a**) and distal (**b**) images of the liver lesion phantom at 100 mAs and 5-mm slice thickness. Images with random opacity location were created by placing a region of interest over the opacity in the central image (**c**) and pasting the opacity onto the distal image (**d**). The opacity circled in **c** and **d** is the 9.5-mm opacity investigated in this study

they typically overestimated the diameter of the 2.4 mm opacities. For observer agreement and sensitivity, binomial data were used, i.e., lesion was visible (observer scores of 2, 3, or 4) or not visible (observer score of 1). For all analyses, findings with $p<0.05$ were considered statistically significant.

Results

Observer Scores

The median and mean observer scores for both random and framed lesions for each slice thickness and exposure combination are listed in Table 1. A difference in median observer score was noted for the 9.5 mm opacity with the 1-mm slice thickness/75mAs exposure combination ($p<0.05$). No other significant differences were observed.

Correlation

There was strong correlation between the observer scores for random and framed lesion location for all opacities ($r=0.92$, $p<0.0001$), for the 9.5 mm opacity ($r=0.96$, $p<0.0001$), and a weaker but still significant correlation for the 2.4 mm opacity ($r=0.64$, $p<0.05$) (Table 2). No significant correlation was shown for the 4.8 mm opacity.

Table 2 Correlation of observer scores for random and framed lesion locations: significant results are indicated by an asterisk

Lesion size	Spearman's rank correlation coefficient (r)	p value
All lesions	0.89	<0.001*
9.5 mm lesion	0.94	<0.0001*
4.8 mm lesion	0.51	0.09
2.4 mm lesion	0.64	<0.05*

Observer Agreement

Observer agreement between the observer scores for each lesion size was good, whether lesions were presented in framed or random location (K range, 0.74–0.96), with the exception of the 4.8-mm opacity size for the framed location condition ($K=0.35$) (Table 3).

Sensitivity

A difference in sensitivity between the framed and randomly located lesions was noted for the 9.5-mm lesion at the 75 mAs/1 mm slice thickness setting ($p<0.05$) and the 4.8-mm lesion at the 75 mAs/3 mm slice thickness setting ($p<0.05$) (Table 4). No other significant differences were noted.

Discussion

The invariance of most proprietary quality assurance phantoms does not replicate the normal clinical setting in which the presence, location, and extent of disease are often unknown prior to the examination. To overcome this potential limitation, computer simulation programs randomizing disease locations have been described: Hoe and colleagues [10] electronically subtracted real lesions from pediatric CT examinations of the liver and used them to create simulated lesions to assist dose optimization of pediatric body CT examinations by providing a larger database, while Hanai and others [17] introduced virtual nodules into the CT

Table 3 Interobserver agreement between mean observer scores for framed and random location methods

Lesion size	Randolph's free marginal kappa (K)	
	Framed opacity location	Random opacity location
All lesions	0.74	0.84
9.5 mm lesion	0.94	0.77
4.8 mm lesion	0.35	0.78
2.4 mm lesion	0.94	0.96

Table 4 Median and mean sensitivity for the three opacity sizes for framed and random location conditions at each exposure/slice thickness setting: *p* value is presented when a significant difference between the two methods exists

Lesion size (mm)	Slice thickness (mm)	Exposure (mAs)	Median (mean) sensitivity		*p* value
			Framed opacity location	Random opacity location	
9.5	5	125	1.00 (1.00)	1.00 (1.00)	
		100	1.00 (1.00)	1.00 (1.00)	
		75	1.00 (1.00)	1.00 (0.96)	
		50	1.00 (1.00)	1.00 (0.96)	
	3	125	1.00 (1.00)	1.00 (1.00)	
		100	1.00 (1.00)	1.00 (1.00)	
		75	1.00 (1.00)	1.00 (0.91)	
		50	1.00 (1.00)	1.00 (0.98)	
	1	125	1.00 (0.98)	1.00 (0.96)	
		100	1.00 (0.96)	1.00 (0.87)	
		75	1.00 (0.96)	0.60 (0.58)	<0.05
		50	1.00 (0.91)	0.80 (0.76)	
4.8	5	125	0.20 (0.27)	0.40 (0.33)	
		100	0.20 (0.27)	0.00 (0.00)	
		75	0.20 (0.24)	0.00 (0.07)	
		50	0.00 (0.13)	0.00 (0.04)	
	3	125	0.20 (0.31)	0.20 (0.20)	
		100	0.20 (0.20)	0.00 (0.02)	
		75	0.40 (0.29)	0.00 (0.07)	<0.05
		50	0.20 (0.24)	0.00 (0.09)	
	1	125	0.20 (0.18)	0.20 (0.13)	
		100	0.00 (0.13)	0.00 (0.02)	
		75	0.00 (0.16)	0.00 (0.04)	
		50	0.00 (0.16)	0.00 (0.04)	
2.4	5	125	0.00 (0.04)	0.00 (0.00)	
		100	0.00 (0.04)	0.00 (0.00)	
		75	0.00 (0.04)	0.00 (0.00)	
		50	0.00 (0.02)	0.00 (0.00)	
	3	125	0.00 (0.00)	0.00 (0.00)	
		100	0.00 (0.00)	0.00 (0.00)	
		75	0.00 (0.00)	0.00 (0.02)	
		50	0.00 (0.00)	0.00 (0.00)	
	1	125	0.00 (0.00)	0.00 (0.00)	
		100	0.00 (0.00)	0.00 (0.00)	
		75	0.00 (0.02)	0.00 (0.04)	
		50	0.00 (0.00)	0.00 (0.00)	

projection data from scans of a proprietary CT lung nodule phantom prior to image reconstruction to provide a more realistic representation of lung malignancies. Although each method was validated as producing simulated lesions indistinguishable from actual lesions, the techniques required customized computer software, image manipulation, and reconstruction of the scan data, indicating that they would be impractical for routine clinical use. Moreover, to our knowledge, the requirement for randomization of disease presence and/or location for CT dose optimization purposes has not been established.

In the clinical setting, the diagnostic task of lesion detection usually involves visual search [18, 19] and a predominance of normal cases [13, 20], elements that are absent in a typical CT optimization methodology involving a phantom with fixed location of lesions. It has been shown that if an observer receives visual cues for the location or presence of an abnormality, sensitivity is increased [21, 22]. In our

study, observer knowledge of lesion location did not alter observer performance when conditions were unambiguous, that is when lesions were either very obvious (9.5 mm) or nonvisible (2.4 mm) to the observers. When conditions were more challenging with the 4.8-mm opacity, there was disagreement between the random- and framed-location results in terms of correlation of scores and interobserver variation. Three decades ago, Kundel et al. [23] demonstrated that inadequate visual search was responsible for approximately 30 % of missed lung nodules on chest X-rays; consequently, it is not surprising that the opacities in the current study were more readily detected with the known lesion presentation. A high level of observer uncertainty may account for the poor interobserver agreement for the 4.8-mm lesion under framed conditions: While the large opacity was clearly noticeable and the small opacity definitely invisible at most settings, the conspicuousness of the intermediate lesion was more ambiguous and some observers may have overestimated their confidence in perceiving this lesion because its location could be accurately determined by adjacent opacities that were plainly visible due to their larger size and/or greater density difference to the background.

Hepatic lesions smaller than 10 mm in diameter are likely to be benign, particularly in patients with no history of malignancy [13, 14, 20]. Our results suggest that the use of a phantom with fixed lesion location may therefore be adequate for optimization of routine liver protocols when the detection of small lesions is not required. However, for individuals with a cancer history, detection and characterization of lesions with a smaller diameter may impact upon their management, and therefore, an optimization process using fixed lesion location may result in exposures that are too low for establishing the most appropriate patient care pathway.

The method of randomizing the opacities presented here is readily reproducible as it utilizes commercially available software; however, the process of cutting and pasting opacities was time consuming, and expert DICOM and PACS advice is required to manage changes to image header information caused by the editing process. To streamline scan protocol optimization for challenging conditions, development of more cost-effective and user-friendly methods is required.

Some degree of caution should be exercised when interpreting our results. Firstly, the opacities and phantom background were homogeneous in their density and perfectly spherical in shape, and only the central image of each scan series was presented, which does not accurately reflect the clinical situation. The purpose of our study, however, was to compare unknown versus known lesion location rather than the absolute accuracy of the optimization process. Secondly, we only considered lesions with density 10 HU lower than that of the background; nevertheless, while lesions with greater difference in density or with higher density to background may have presented different results, a 10-HU density difference represents the minimum lesion-to-liver contrast necessary for detection [24, 25]. Finally, the study was performed on one scanner, and care must be exercised in extrapolating these results to other scanner models.

Conclusions

Optimizing CT hepatic examinations using phantoms requires randomized lesion location when investigating challenging conditions such as small lesion detection; however, a standard phantom with fixed lesion location is suitable for the optimization of routine liver protocols.

Acknowledgments This research was supported by the Medical Radiation Technologists' Board Queensland, the Australian Institute of Radiography, the University of Sydney Faculty of Health Sciences, the Royal Brisbane and Women's Hospital Department of Medical Imaging Research Fund, and Queensland Health. We thank the nine observers, Liam Caffery, Frank Carbon, and Mark Bartlett for their assistance with DICOM issues, and Peter O'Rourke and Lee Jones for statistical advice.

References

1. Wise K, Thomson J: Changes in CT radiation doses in Australia from 1994–2002. The Radiographer 51:81–85, 2004
2. Kaul A, Bauer B, Bernhardt J, Nosske D, Veit R: Effective doses to members of the public from the diagnostic application of ionizing radiation in Germany. Eur Radiol 7:1127–1132, 1997
3. Mettler Jr, FA, Wiest PW, Locken JA, Kelsey CA: CT scanning: patterns of use and dose. J Radiol Prot 20:353–359, 2000
4. Hart D, Wall B: Radiation exposure of the UK population from medical and dental x-ray examinations. Chilton: National Radiological Protection Board, Report No. NRPB-W4, 2002
5. Aroua A, Burnand B, Decka I, Vader JP, Valley JF: Nation-wide survey on radiation doses in diagnostic and interventional radiology in Switzerland in 1998. Health Phys 83:46–55, 2002
6. Bongartz G, Golding SJ, Jurik A, Leonardi M, van Persijn van Meerten E, Rodriquez R, Schneider K, Calzado A, Geleijns A, Jessen J, Panzer KA, Shrimpton PC, Tosi G: European Guidelines for multislice computed tomography. European Commission, contract no. FIGM-CT2000-20078-CT-TIP, 2004
7. Cohnen M, Poll LJ, Puettmann C, Ewen K, Saleh A, Modder U: Effective doses in standard protocols for multi-slice CT scanning. Eur Radiol 13:1148–1153, 2003
8. International Commission on Radiological Protection: The 2007 Recommendations of the International Commission on Radiological Protection. ICRP publication 103. Ann. ICRP 37, 1–332, 2007
9. Rusinek H, Naidich DP, McGuinness G, Leitman BS, McCauley DI, Krinsky GA, Clayton K, Cohen H: Pulmonary nodule detection: low-dose versus conventional CT. Radiology 209:243–249, 1998
10. Hoe CL, Samei E, Frush DP, Delong DM: Simulation of liver lesions for pediatric CT. Radiology 238:699–705, 2006

11. Li X, Samei E, Delong DM, Jones RP, Gaca AM, Hollingsworth CL, Maxfield CM, Carrico CW, Frush DP: Three-dimensional simulation of lung nodules for paediatric multidetector array CT. Br J Radiol 82:401–411, 2009
12. Starr SJ, Metz CE, Lusted LB, Goodenough DJ: Visual detection and localization of radiographic images. Radiology 116:533–538, 1975
13. Schwartz LH, Gandras EJ, Colangelo SM, Ercolani MC, Panicek DM: Prevalence and importance of small hepatic lesions found at CT in patients with cancer. Radiology 210:71–74, 1999
14. Robinson PJ, Arnold P, Wilson D: Small "indeterminate" lesions on CT of the liver: a follow-up study of stability. Br J Radiol 76:866–874, 2003
15. Winterer JT, Kotter E, Ghanem N, Langer M: Detection and characterization of benign focal liver lesions with multislice CT. Eur Radiol 16:2427–2443, 2006
16. Brennan PC, McEntee M, Evanoff M, Phillips P, O'Connor WT, Manning DJ: Ambient lighting: effect of illumination on soft-copy viewing of radiographs of the wrist. Am J Roentgenol 188:W177–W180, 2007
17. Hanai K, Horiuchi T, Sekiguchi J, Muramatsu Y, Kakinuma R, Moriyama N, Tuchiiya R, Niki N: Computer-simulation technique for low dose computed tomographic screening. J Comput Assist Tomogr 30:955–961, 2006
18. Tuddenham WJ: Visual search, image organization, and reader error in roentgen diagnosis. Studies of the psycho-physiology of Roentgen image perception. Radiology 78:694–704, 1962
19. Donovan T, Manning DJ: The radiology task: Bayesian theory and perception. Br J Radiol 80:389–391, 2007
20. Jones EC, Chezmar JL, Nelson RC, Bernardino ME: The frequency and significance of small (less than or equal to 15 mm) hepatic lesions detected by CT. Am J Roentgenol 158:535–539, 1992
21. Kinchla RA, Chen Z, Evert D: Precue effects in visual search: data or resource limited? Percept Psychophys 57:441–450, 1995
22. Solomon JA: The effect of spatial cues on visual sensitivity. Vision Res 44:1209–1216, 2004
23. Kundel HL, Nodine CF, Carmody D: Visual scanning, pattern recognition and decision-making in pulmonary nodule detection. Invest Radiol 13:175–181, 1978
24. Baron RL: Understanding and optimizing use of contrast material for CT of the liver. Am J Roentgenol 163:323–331, 1994
25. Foley WD, Berland LL, Lawson TL, Smith DF, Thorsen MK: Contrast enhancement technique for dynamic hepatic computed tomographic scanning. Radiology 147:797–803, 1983